# Binding of Glyco-Acridine Derivatives to Lysozyme Leads to Inhibition of Amyloid Fibrillization

Quan Van Vuong,[†] Katarina Siposova,[‡,§] Trang Truc Nguyen,[†] Andrea Antosova,[‡] Lucia Balogova,[∥] Ladislav Drajna,[§] Jan Imrich,[§] Mai Suan Li,[⊥] and Zuzana Gazova*,[‡]

[†]Institute for Computational Science and Technology, 6 Quarter, Linh Trung Ward, Thu Duc District, Ho Chi Minh City, Vietnam
[‡]Department of Biophysics, Institute of Experimental Physics, Slovak Academy of Sciences, Watsonova 47, 040 01 Kosice, Slovakia
[§]Institute of Chemistry, [∥]Department of Biophysics, Faculty of Science, P. J. Safarik University, Srobarova 2, 041 54 Kosice, Slovakia
[⊥]Institute of Physics, Polish Academy of Sciences, Al. Lotnikow 32/46, 02-668 Warsaw, Poland

**S** *Supporting Information*

**ABSTRACT:** While amyloid-related diseases are at the center of intense research efforts, no feasible cure is currently available for these diseases. The experimental and computational techniques were used to study the ability of glyco-acridines to prevent lysozyme amyloid fibrillization in vitro. Fluorescence spectroscopy and atomic force microscopy have shown that glyco-acridines inhibit amyloid aggregation of lysozyme; the inhibition efficiency characterized by the half-maximal inhibition concentration $IC_{50}$ was affected by the structure and concentration of the derivative. We next investigated relationship between the binding affinity and the inhibitory activity of the compounds. The semiempirical quantum PM6-DH+ method provided a good correlation pointing to the importance of quantum effects on the binding of glyco-acridine derivatives to lysozyme. The contribution of linkers may be explained by the valence bond theory. Our data provide a basis for the development of new small molecule inhibitors effective in therapy of amyloid-related diseases.
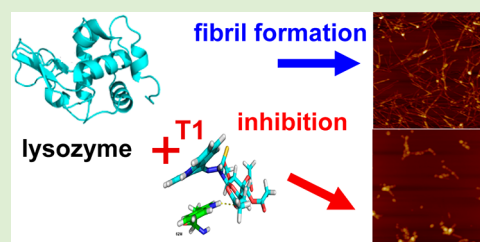
## 1. INTRODUCTION

Alzheimer's disease, prion disorders, amyotrophic lateral sclerosis, and type 2 diabetes are associated with the presence of protein amyloid deposits.[1,2] In fact, more than 25 different human poly/peptides can form intra- or extracellular amyloid aggregates in various tissues that are associated with either systemic or localized amyloidosis. Proteins undergo major conformational changes leading to formation of amyloid aggregates (dimers, oligomers, pores, protofilaments, fibrils) by a nucleated growth polymerization pathway where the intermolecular interactions are favored over the intramolecular ones.[3,4]

Although amyloidogenic proteins demonstrate no sequence or structural homology, amyloid aggregates do exhibit common structural and immunogenic properties as well as cytotoxicity. The precise mechanism by which the protein amyloid elicits cell damage remains elusive. It is still a matter of debate, which type of amyloid aggregates is the predominant pathogenic species. Present evidence claim that toxicity can result from deposition of huge fibril assemblies in the tissues causing the organ failure. Recent data suggest that soluble amyloid aggregates are predominant pathogenic species due to their direct interaction with the membrane inducing the inappropriate membrane permeabilization and subsequent cell death.[5,6]

Taking into account that protein amyloid aggregation is the multistep process, several therapeutic approaches to treat amyloidosis have been suggested.[7] A direct inhibition of the protein amyloid formation[8] or clearance of amyloid fibrillar assemblies appear to be promising therapeutic interventions.[9] Therefore, considerable efforts are being devoted to the development of new antiaggregating agents.

Small molecules are good drug candidates due to their ability to cross cell membranes and the blood−brain barrier relatively easily. It was shown that small aromatic molecules are efficient inhibitors of amyloid fibril formation in vitro[10,11] and can prevent the cell death in amyloidogenic cytotoxicity assays.[12,13] Although many details regarding their mechanisms of action remain obscure, it was suggested that disruption of hydrophobic and $\pi$-stacking interactions of aromatic residues are involved.[14−16] Aromatic compounds, such as rottlerin, clotrimazole, or sulconazole, interfere with amyloidogenesis of prion proteins and lysozyme.[17,18] DeFelice et al. described antiamyloidogenic and neuroprotective action of some di- and trisubstituted aromatic compounds.[19] Curcumin inhibits the aggregation of a Abeta peptide, $\alpha$-synuclein,[20,21] and lysozyme.[22] Catecholamines such as dopamine disaggregate fibrils of a Abeta and $\alpha$-synuclein after a 1 day incubation.[23] Bahramikia et al. have shown that salen−manganese complexes disperse the lysozyme fibrillar aggregates in a dose-dependent manner.[24] Several small polyphenol molecules remarkably inhibit the formation of fibrillar assemblies in vitro and decrease their cytotoxicity.[10] Among nitrogen aromatic

structures, the indole derivatives were found to inhibit amyloid fibril formation of Abeta peptide depending on their structure.[25] For example, indole-3-acetic acid effectively diminished the hen egg-white lysozyme amyloid fibrillization and disaggregated preformed amyloid fibrils.[26] We have previously demonstrated the structure-related activity of a diverse aromatic acridine derivatives toward the aggregation of the lysozyme in vitro.[27,28]

Recent data indicate that even proteins not associated with any known amyloid diseases can form amyloid aggregates in vitro, with structure and toxicity similar to amyloids formed by disease-related proteins.[29,30] These findings suggest that ability to form amyloid aggregates is a rather generic property of polypeptide chains regardless of their source, sequence, or tertiary structure.[3,31] The study of amyloid aggregation of proteins not directly associated with amyloidogenic disease could therefore shed more light on our understanding of aggregation process and reveal ways to disrupt them.

Hen egg-white lysozyme (HEWL) is one of the proteins most explored in the aggregation studies thanks to the wealth of data about its three-dimensional structure, folding, and stability.[32,33] The hen protein is structurally highly homologous (40%) to human lysozyme, whose different variants (Ile56Thr and Asp67His) form massive amyloid deposits in the liver and kidneys of the individuals affected by a hereditary systemic amyloidosis.[34,35] Recent in vitro studies have shown that HEWL undergoes the amyloid aggregation, that is, destabilization of the native structure under partially denaturing conditions (acid pH, high temperature, presence of denaturants), which increase an aggregation-prone protein population.[36,37] Based on these findings, HEWL became an ideal model system to study protein amyloid aggregation.

In this study, we investigated the interference of glyco-acridine derivatives with amyloid aggregation of the HEWL in vitro. Our results indicate that glyco-acridines prevent amyloid fibrillization, and the extent of the inhibitory activity depends on compound concentration and structure. In addition, we studied the binding affinity of glyco-acridines using a classical docking and semiempirical quantum-mechanical PM6-D H+ methods. Our studies revealed that hydrogen bonding is not the key factor controlling the binding affinity and underscore the role of van der Waals and electrostatic interactions, which are dependent on the structure of the compounds.

## 2. EXPERIMENTAL SECTION

**2.1. Chemicals.** Lysozyme from chicken egg white (CEW lysozyme, E.C. number: 3.2.1.17, lyophilized powder, L 6876, ~50000 units mg$^{-1}$ protein), NaCl, Congo red (CR), and thioflavin T (ThT) were obtained from Sigma Chemical Company (St. Louis, MO). All other chemicals were purchased from Sigma or Fluka and were of analytical reagent grade. The protein concentrations were determined spectrophotometrically (Specord S100, Analytik Jena) using extinction coefficient at $\lambda = 280$ nm of 2.63 L·g$^{-1}$·cm$^{-1}$. Studied acridine derivatives were synthesized in the Department of Organic Chemistry, Faculty of Science, P. J. Safarik University in Kosice. Glyco-acridines stock solutions were prepared in DMSO and samples were freshly prepared by dilution of stocks immediately before the measurements (DMSO content in measured samples was lower than 2%).

**2.2. Lysozyme Amyloid Fibrillization.** Lysozyme was dissolved to a final concentration of 10 $\mu$M in 70 mM glycine buffer (pH 2.7) containing 80 mM NaCl. The solution was incubated for 2 h at 65 °C under constant stirring (1200 rpm). The formation of lysozyme aggregates was monitored by ThT and CR assays, circular dichroism spectroscopy, and atomic force microscopy (AFM).

**2.3. Thioflavin T (ThT) Fluorescence Assay.** The lysozyme fibril formation was monitored by a characteristic increase in ThT fluorescence intensity. ThT was added to lysozyme samples (10 $\mu$M) to a final concentration of 20 $\mu$M and samples were incubated at 37 °C for 1 h. The fluorescence intensity was measured using a spectrofluorimeter Shimadzu RF-5000 with the excitation set to 440 nm and the emission recorded at 485 nm. Fluorescence measurements were performed in a semimicro-quartz cuvette with 1 cm excitation light path; slits were adjusted to 1.5 and 3.0 nm for the excitation and the emission, respectively.

**2.4. AFM Measurements.** Samples for AFM were prepared by a drop casting of the solution on the surface of freshly cleaved mica. After 2 min adsorption, samples were rinsed with ultrapure water and left to dry prior to scan. The protein concentration was always 10 $\mu$M and concentration of glyco-acridines was 200 $\mu$M. AFM images were taken by a Scanning Probe Microscope (Veeco di Innova, Bruker AXS Inc., Madison, U.S.A.) in a tapping mode under ambient conditions using uncoated silicon cantilevers NCHV (Bruker AFM Probes, Camarillo, U.S.A.) with nominal resonance frequency 320 kHz and spring constant 42 N/m. All images are unfiltered.

**2.5. Screening of Glyco-Acridines Mediated Inhibition of Lysozyme Amyloid Fibrillization.** The ThT assay was used to evaluate the ability of the studied compounds to inhibit the lysozyme amyloid fibrillization. The glyco-acridine derivative (200 $\mu$M, final concentration) was added to lysozyme solution (10 $\mu$M). The solution was exposed to amyloid aggregation inducing conditions described above. In the control experiment, the protein was omitted to measure the fluorescence of glyco-acridines. Each experiment was performed in triplicate and the presented value is the average of the three measured values.

**2.6. Determination of IC$_{50}$.** The IC$_{50}$ values were determined by measuring the extent of inhibition of the formation of amyloid aggregates by glyco-acridine derivatives at concentrations between 10 pM and 1 mM and fixed 10 $\mu$M protein concentration. The extent of aggregation was observed by the ThT assay. The fluorescence intensities were normalized to the fluorescence signal of amyloid aggregates alone. Each experiment was performed in triplicate and the final value is the average of the measured values. The IC$_{50}$ values were determined from dose–response curves obtained by fitting the average values by nonlinear least-squares method. The volume of DMSO in measure samples was lower than 2% and had no effect on the formation or the stability of lysozyme fibrils.

**2.7. Docking Method.** The lysozyme structure (193L) was obtained from the RSCB Protein Data Bank. Protonation at pH 2.7 was calculated by a PDB2PQR server[38] with the Amber force field. We used AutodockTools 1.5.4[39] to prepare the PDBQT file for the lysozyme and ligands. The PDBQT files were used as the input for the Autodock Vina version 1.1,[40] which is more efficient than Autodock 4 to dock various ligands to lysozyme. A modified version of the CHARMM force field[41,42] was implemented to discern the atomic interactions. In Autodock Vina, the Broyden–Fletcher–Goldfarb–Shanno method[43] was employed for local optimization. To obtain accurate results, we set the exhaustiveness of global search equal to 1000. The maximum energy difference between the worst and best binding modes was chosen to be 7. A total of 10 binding modes (10 modes of docking) were generated with random starting positions of the ligand which has fully flexible torsion degrees of freedom. The center of grids was placed at the center of mass of the receptor. Grid dimensions were chosen large enough to cover the whole receptor.

**2.8. PM6-DH+ Method.** The docking method neglects a dynamics of the receptor and thus cannot account for the deformation energy deflections resulting from the ligand conformation changes during the docking trials. In addition, it does not incorporate important quantum effects such as charge transfer between the receptor and the ligand, the change of atomic charge upon ligand binding, and bonding of X–H to $\pi$ bonds (X = O, N). To overcome these shortcomings, one can use more accurate quantum mechanical methods such as HF, DFT, and so on. However, those methods are very CPU–time-consuming even for a small system. In this situation, one of reasonable ways to deal with large systems like biomolecules is to use the semiempirical quantum

mechanical method PM6,[44,45] which is accurate enough but computationally not as expensive. However, PM6 still has some problems with the description of dispersion and hydro-bonding interactions. These drawbacks have been remedied in the recently improved PM6-DH+ version of this method.[46,47] Thus, we will use PM6-DH+ for optimizing and rescoring structures obtained from docking. The binding energy was calculated from the standard equation.

$$\Delta E_{bind} = E_{R+L} - E_R - E_L \tag{1}$$

where $E_{R+L}$, $E_R$, and $E_L$ are total energies of the receptor—ligand complex, free receptor, and free ligand, respectively. PM6-DH+ provides interaction parameters in such a way that it reproduces interaction energies for geometries obtained from high-level quantum mechanical calculation.[45] All MP6-DH+ calculations were conducted using a MOPAC-2009 package[45] where mozyme algorithm was based on the localized orbital, a linear scaling technique. This allowed a substantial reduction of CPU time.[47,48]

For each ligand, 10 lowest energy conformations of the protein—ligand complexes obtained from docking were chosen for further calculations. A H atom and Cl⁻ ion were added to neutralize the system by a AMBER—ff99SB and gaff force field implemented in a TLEAP package.[49] Conformations were also optimized by the PM6-DH+ method and mozyme algorithm in a continuum COSMO solvent model[45,50] with parameters rsolv = 1.3, nspa = 122, and $\varepsilon$ = 78.4. For optimization we used a criterion rmsGrad = 3 kcal/mol/Å. In the last stage, the total energy was estimated by the PM6-DH+ method without mozyme algorithm to obtain higher accuracy. The protein structure was treated in the same way as the protein—ligand complex.

To find a stable conformation for the isolated ligand, a lot of initial conformations have been generated by varying dihedral angles of all rotatable bonds. This way, obtained initial conformations were optimized by calculating the total energy by PM6-DH+ method without mozyme algorithm in the continuum COSMO solvent model. The stable conformation of the ligand was the one with the lowest energy.

**2.9. Hydrogen Bond and Side Chain Contacts.** Hydrogen bond (HB) and side chain contacts (SC) were studied to reveal the nature of the ligand binding. HB is formed when the distance between donor D and acceptor A is ≤3.5 Å and the D—H—A angle is ≥135°. SC contact is considered to be formed if the distance between the ligand atom and the center of mass of the residue side chain is ≤6.5 Å.

## 3. RESULTS AND DISCUSSION

The recent studies, which suggested that prevention of protein amyloid aggregation could alleviate the symptoms of incurable amyloid-related diseases, generated a strong interest to find new compounds aimed to inhibit the amyloid fibrillization. We have investigated the ability of nine glyco-acridine derivatives to decrease the amyloid aggregation of hen egg white lysozyme, the model amyloidogenic protein, in vitro. To pinpoint the most effective derivatives with a therapeutic potential, we examined their binding affinity in order to understand the mechanism of their inhibition of amyloid polymerization.

**3.1. Amyloid Fibrillization of Lysozyme.** Lysozyme amyloid aggregates were obtained by incubation of the soluble protein in saline solution for 2 h under acidic conditions and constant stirring. The formation of amyloid aggregates was confirmed by two independent methods: ThT fluorescence assay and atomic force microscopy. Binding of ThT to assembled $\beta$-structures of amyloid fibrils significantly increased fluorescence intensity of ThT that was not detected for the native protein (Figure 1A). Formation of amyloid fibrils was also observed as shift of the absorbance maximum of Congo red in the presence of fibrils and increasing of the $\beta$-sheet contents determined by CD spectroscopy (Supporting Information, Figure S1). Visualization of the lysozyme aggregates by AFM confirmed the typical morphology of the
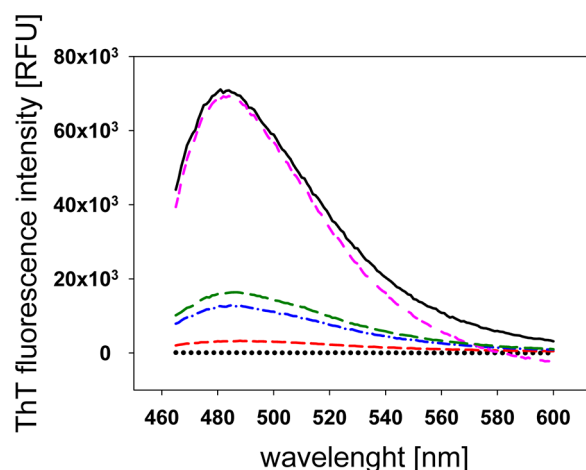


**Figure 1.** ThT fluorescence spectra of lysozyme native (10 $\mu$M; black dots), lysozyme after fibrillization in the absence (solid black line) or presence of 200 $\mu$M glycoacridines T2 (red dash line), C1 (blue dash-dot line), I2 (green long dash line), and S1 (violet dash-dot-dot line).

amyloid fibrils (Figure 2A); the thicker species arose by a lateral association of the fibrils.

**3.2. Glyco-Acridines.** Investigated derivatives of glyco-acridine were synthetized in our laboratory[38] and are composed of a planar tricyclic acridin-9-yl core and a side saccharide chain connected by a linker. Saccharide terminal units contain tetra-acetylated or nonacetylated $\beta$-D-glucopyranosyl or $\beta$-D-galactopyranosyl skeletons. Four types of linkers have been prepared based on a starting 9-hydrazinoacridine and 2,3,4,6-tetra-O-acetyl-$\beta$-D-glycopyranosylisothiocyanate synthons (Glu = 1, Gal = 2): thiosemicarbazides (T), semicarbazides (S), isothiosemicarbazides (I), and cyclic 1,3-thiazolidinones (C). The availability of central linkers with various bulkiness and heteroatoms, such as nitrogen, sulfur, and oxygen, allowed us to study the relationship between the chemical structure and inhibition of lysozyme fibrillization. The chemical structures of all screened compounds are shown in Table 1.

**3.3. Inhibition of Lysozyme Fibrillization by Glyco-Acridine Derivatives.** In the primary screen of inhibitory activity of 200 $\mu$M glyco-acridines on the lysozyme fibrillization, the extent of lysozyme aggregation was quantified by the ThT fluorescence assay. As expected the ThT signal intensity correlated with the amount of protein with the amyloid cross-$\beta$ structure. Addition of tested compounds affected the lysozyme amyloid polymerization quite differently. A significant decrease of ThT fluorescence to values lower than 50% of the control sample, which indicated important prevention of the lysozyme fibrillization, was detected for compounds from the thiosemi-carbazide, isothiosemicarbazide, and cyclic 1,3 thiazolidinone subclasses. The presence of semicarbazide carbonyls in linkers of S1 and S2 led to a significant drop of the inhibitory activity; none or minimal (about 5%) decrease of ThT fluorescence was observed. Representative results of primary screening of each structural subclass of glyco-acridines are shown in Figure 1.

AFM images confirmed that changes in the shape and amount of amyloid aggregates depend on the structure of the compound, as suggested by the ThT fluorescence assay. The extensive reduction of fibrillar aggregates was detected in the presence of compounds C1 and I1 (Figure 2B,C) when compared with the aggregates produced by protein alone (Figure 2A). The aggregates produced in the presence of these effective derivatives appeared less fibrillar and more amorphous
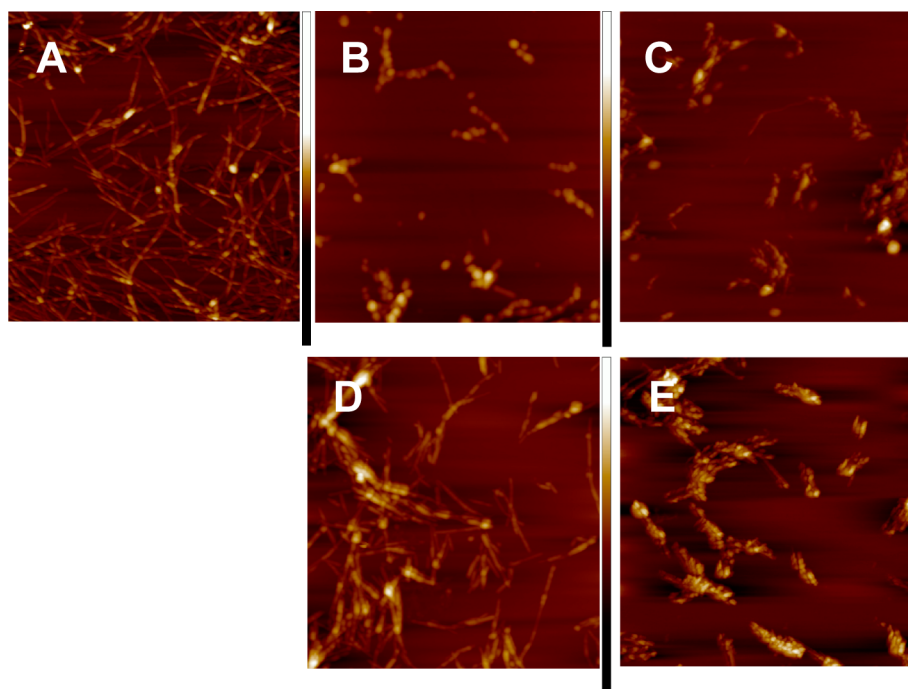
**Figure 2.** AFM images of lysozyme solution obtained after the process inducing the protein fibrillization in the absence (A) and presence of 200 $\mu$M glyco-acridine derivatives C1 (B), I1 (C), S1 (D), and T1OH (E). The scan size is 5 × 5 $\mu m^2$ in all images.

in comparison with untreated fibrils. Lower inhibitory activity was detected with deacetylated T1OH derivative (Figure 2E), whereas the amount of amyloid self-assemblies in the presence of the S1 derivative (Figure 2D), possessing a C=O group in the linker, was the same as that observed for protein alone (Figure 2A). Thus, retention of the morphology of the amyloid fibrils formed in the presence of semicarbazide compounds suggests that they lack inhibitory activity toward fibrillization of lysozyme.

**3.4. Determination of IC$_{50}$ Values.** To obtain more precise data about the inhibitory ability of the studied compounds, the half-maximal inhibition concentrations, IC$_{50}$, were determined for all active compounds (except S1) by the ThT fluorescence assay. All active glyco-acridine derivatives inhibited the lysozyme polymerization in a concentration-dependent manner. Typical curves of representative acridines from each glycol-acridine subclass (T2, C1, I2, and S2) in concentration range $10^{-3}$ to $10^{-10}$ M are shown in Figure 3. The IC$_{50}$ values obtained from those curves are summarized in Table 2. All IC$_{50}$ values are in the micromolar range and comparable to protein concentration with the exception of S2 (133 $\mu$M); the lowest IC$_{50}$ values were obtained for cyclic thiazolidinones C1, C2 (0.26 and 4.17 $\mu$M), and thiosemi-carbazide acridines T1, T2 (4.45 and 9.47 $\mu$M). All the results presented thus far suggest that the most effective compounds exhibit inhibitory activity at sub/stoichiometric concentrations. We have thus found that the structure of glyco-acridines is an important factor determining their inhibitory ability. In light of these findings, we conclude that the presence of tricyclic acridine core is crucial because the high antiamyloid activity was previously observed especially with ring structure compounds, particularly in relation to aggregation of Abeta peptide and transthyretin.[11,12,51] Moreover, another contributing factors may be (a) the planarity of the heterocyclic skeleton of acridine derivatives, which can block intermolecular protein interactions leading to aggregation, and (b) the structure of the opposite moiety and the linker as well.

The obtained results support the recent evidence that molecule structure is an important factor determining their efficiency to inhibit amyloid aggregation. Aromatic-rich compounds, especially polyphenolic small molecules were described as efficient in vitro inhibitors of amyloid fibril formation with IC$_{50}$ values in the range 1−50 $\mu$M.[52] The tannic acid was found the most potent inhibitor with an IC$_{50}$ value of 0.1 $\mu$M. It was assumed that inhibition of amyloid formation is not dependent on antioxidative properties of polyphenols and can be explained by (a) specific structural conformation necessary for $\beta$-sheet interaction and stabilization of the inhibition−protein complex and (b) aromatic interaction between the phenolic compound in the inhibitor molecule and aromatic residues in the amyloidogenic sequence, which may direct the inhibitor to the amyloidogenic core and interfere with fibril assembly.

On the other hand, the radical scavenging activity and autoxidation of polyphenols together with aromatic and hydrophobic interactions were suggested to be the major reasons for (−)-epicatechin gallate being the most effective inhibitor of lysozyme fibrillization.[53] Weak forces between inhibitor and peptide chains, including hydrogen bonding and hydrophobic and aromatic interactions, have been suggested to be the driving forces in the antiamyloidogenic role of polyphenols.[54,55]

Recently, we have found that structure of tricyclic core of various acridine derivatives represents important structural requirement affecting their antiamyloid activities.[28] The flat heterocyclic skeleton of the planar acridine allows it to intercalate between the hydrophobic residues, thereby inter-rupting the interface between the two neighboring $\beta$-sheets of misfolded lysozyme proteins. Since the compound with the lowest IC$_{50}$ of 6.5 $\mu$M was the acridine dimer, it was proposed that the duplication of heterocycles simply increases the

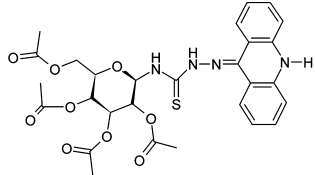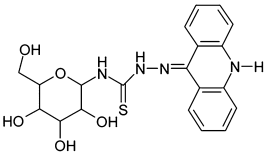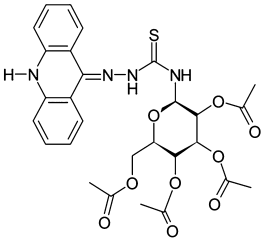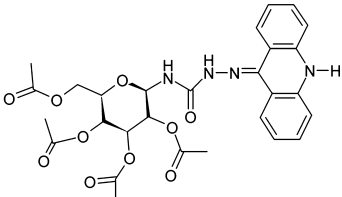**Table 1. Chemical Composition and Formula of Studied Glyco-Acridines**
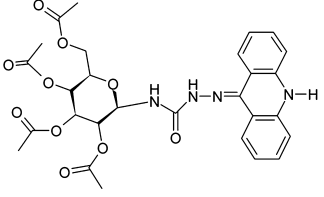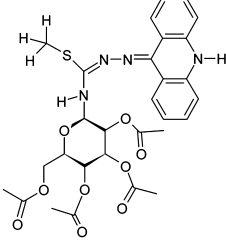


**Thiosemicarbazides**

**T1**
4-(2,3,4,6-Tetra-O-acetyl-β-D-glucopyranosyl)-1-(9,10-dihydroacridin-9-ylidene)thiosemicarbazide

**T1OH**
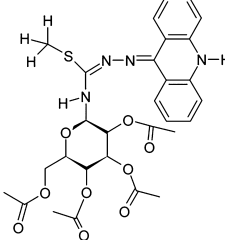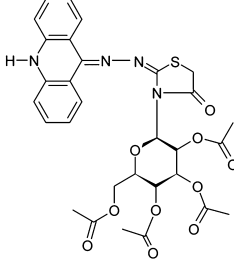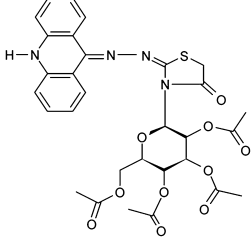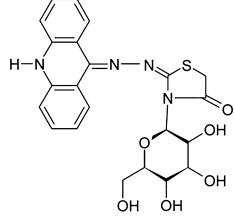4-(β-D-Glucopyranos-1-yl)-1-(9,10-dihydroacridin-9 ylidene)thiosemicarbazide

**T2**
4-(2,3,4,6-Tetra-O-acetyl-β-D-galactopyranosyl)-1-(9,10-dihydroacridin-9-ylidene)thiosemicarbazide

**Semicarbazides**

**S1**
4-(2,3,4,6-Tetra-O-acetyl-β-D-glucopyranosyl)-1-(9,10-dihydroacridin-9-ylidene)semicarbazide

**S2**
4-(2,3,4,6-Tetra-O-acetyl-β-D-galactopyranosyl)-1-(9,10-dihydroacridin-9-ylidene)semicarbazide

**Isothiosemicarbazides**

**I1**
S-Methyl-1-(9,10-dihydroacridin-9-ylidene)-4-(2,3,4,6-tetra-O-acetyl-β-D-glucopyranosyl)isothiosemicarbazide

**I2**
S-Methyl-1-(9,10-dihydroacridin-9-ylidene)-4-(2,3,4,6-tetra-O-acetyl-β-D-galactopyranosyl)isothiosemicarbazide

**Table 1. continued**

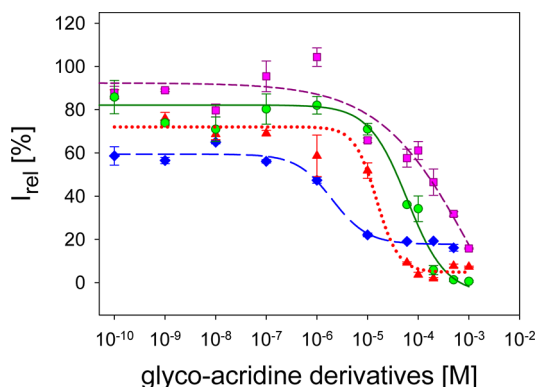| | |
|---|---|
| **Cyclic 1,3-thiazolidinones** | **C1**<br>2′-(9,10-Dihydroacridin-9-ylidene)hydrazono-3′-(2,3,4,6-tetra-*O*-acetyl-*β*-D-glucopyranosyl)-1′,3′-thiazolidin-4′-one |
| **C2**<br>2′-(9,10-Dihydroacridin-9-ylidene)hydrazono-3′-(2,3,4,6-tetra-*O*-acetyl-*β*-D-galactopyranosyl)-1′,3′-thiazolidin-4′-one | **C2OH**<br>2′-(9,10-Dihydroacridin-9-ylidene)hydrazono-3′-(*β*-D-galactopyranos-1-yl)-1′,3′-thiazolidin-4′-one |

**Figure 3.** Determination of $IC_{50}$ values of glyco-acridines by ThT assay; T2 (red triangles), C1 (blue diamonds), I2 (green circles), and S2 (violet squares). The effect of increasing acridine concentrations on lysozyme fibrillization was quantified by normalizing fluorescence intensity to the control (100% fluorescence intensity of the lysozyme aggregates in the absence of compound). A single experiment was performed with each sample in triplicates. The error bars represent the average deviation for repeated measurements of three separate samples. The curves were obtained by fitting of the average values by nonlinear least-squares method.

capacity of the compound to interact with protein, leading to a more effective blockage of *β*-sheet formation. This theory was supported by the decreasing of inhibiting activity due to the loss of core planarity. Data reported by Liu et al. point to the importance of the structure of curcumin, a nonflavonoid polyphenol containing two aromatic phenol subunits, in its ability to suppress the amyloid polymerization of lysozyme in vitro.[56] Curcumin's structure influenced by its thermostability strongly determined the extent of lysozyme fibrillization.

Moreover, formation of dimeric curcumin species significantly increased the inhibitory potency of this compound.

Inhibitory effect of small heterocyclic molecules of imidazole class on the amyloidogenesis of proteins was explained by reduction of the unfolding rates of the aggregation prone state of protein validating the hypothesis of possible thermodynamic mechanism of inhibition due to increasing the energy barrier between the aggregation prone state and the aggregated state.[57] Scherzer-Attali et al. found that quinone−tryptophan hybrids are capable of inhibiting the amyloid aggregation of various poly/peptides such as Abeta, *α*-synuclein, lysozyme, and insulin.[58] Presence of some benzofuranone derivatives at micromolar concentration caused inhibition of insulin amyloid aggregation.[59] A lot of effective small molecule inhibitors of amyloid aggregation that bind and thus stabilize the proteins preventing them from aggregating are reviewed by Gavrin et al.[60]

**3.5. Docking Results.** To study the mechanism of the inhibitory effect in more details, we carried out several modeling experiments. The studied glyco-acridine ligands were docked into a PDB structure of lysozyme. A typical conformation of receptor−ligand complex in the best docking pose corresponding to the lowest binding energy, $\Delta E_{bind}$, is shown in Supporting Information, Figure S2. The minimal binding energies, $E_{binding}$, of nine ligands are listed in Table 2. The binding pocket is formed by residues E35, N46, T47, D48, S50, D52, L56, Q57, I58, N59, R61, W62, W63, I98, D101, N103, N106, A107, W108, V109, A110, R112, and N113.

However, the correlation between binding energies obtained by docking and the experimentally determined $IC_{50}$ values is very poor (correlation coefficient $R = 0.23$; Figure 4, top panel). For example, the ligand C1 has the lowest $IC_{50}$, but its binding energy is among the highest. The poor correlation

**Table 2. IC$_{50}$ Values, Binding Energies, $E_{binding}$, Obtained by Docking and PM6-DH+ Methods; HBs and SC Contacts were Obtained from the Best Docking Pose**

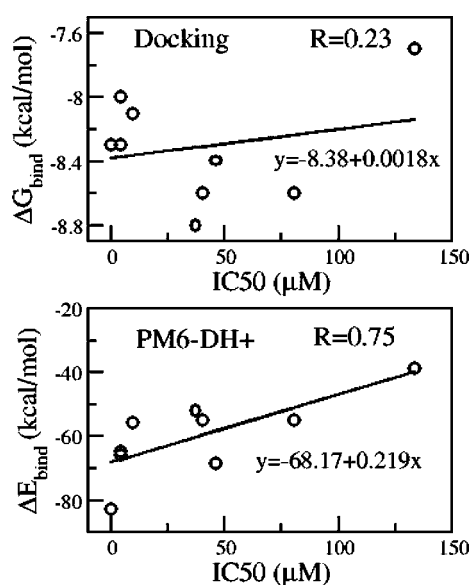| | | docking method | | | PM6-DH+ method | | |
|---|---|---|---|---|---|---|---|
| ligand | IC$_{50}$ ($\mu$M) | $E_{binding}$ (kcal/mol) | H-bonds | SC contacts | $E_{binding}$ (kcal/mol) | H-bonds | SC contacts |
| T1 | 4.45 | −8.0 | 1 | 14 | −65.9 | 6 | 17 |
| T1OH | 80.58 | −8.6 | 3 | 16 | −55.0 | 5 | 11 |
| T2 | 9.47 | −8.1 | 5 | 17 | −56.0 | 4 | 18 |
| S1 | N/A | | | | | | |
| S2 | 133.35 | −7.7 | 3 | 13 | −38.7 | 2 | 17 |
| I1 | 40.31 | −8.6 | 3 | 17 | −55.0 | 6 | 14 |
| I2 | 46.13 | −8.4 | 2 | 16 | −68.6 | 3 | 15 |
| C1 | 0.26 | −8.3 | 4 | 14 | −82.7 | 5 | 17 |
| C2 | 4.17 | −8.3 | 3 | 15 | −64.7 | 4 | 14 |
| C2OH | 37.47 | −8.8 | 4 | 12 | −52.0 | 3 | 12 |



**Figure 4.** Correlation between IC$_{50}$ values and binding energies obtained by docking (top panel) and PM6-DH+ method (bottom panel).

between experimentally obtained IC$_{50}$ and binding energies $E_{bind}$ is not surprising because docking involves a number of crucial approximations including the omission of receptor dynamics and limited numbers for ligand positions in the trial.

**3.6. PM6-DH+ Results.** *Importance of Quantum Effects.* Since the docking approach provided poor correlation of IC$_{50}$ values with the binding affinity, we applied a more sophisticated PM6-DH+ method in which quantum effects were taken into account. The correlation between $\Delta E_{bind}$ obtained by this method and experimental values of IC$_{50}$ is much better ($R$ = 0.75) (Figure 4, bottom panel). This result confirms that PM6-DH+ method is more suitable for modeling of interactions than classical docking and suggest that quantum effects may be important in binding of glyco-acridines to lysozyme.

*Hydrogen Bonding Is Not the Key Factor in the Binding Affinity.* Positions of ligands inside the binding pocket calculated by docking and PM6-DH+ method are not identical (see, for example, Supporting Information, Figure S3) and provide a different number of H bonds (HBs) and SC contacts (Table 2). For T1, C1, C2, T1OH, I1, and I2, the number of HBs with the receptor in PM6-DH+ configurations is larger than that from classical docking. In particular, the docking method affords only one HB between the ligand T1 and the

receptor contrary to six HBs obtained by the PM6-DH+ method (Supporting Information, Figure S4). However, for compounds T2, C2OH, and S2 the quantum effects reduced the number of HBs. In the case of T1, T2, C1, and S2, the PM6-DH+ method gave more SC contacts than docking, while C2OH had an equal number of SC contacts from both approaches (Supporting Information, Figure S5).

There was a negligible correlation between the binding energies obtained by PM6-DH+ method and the numbers of HBs and SC contacts (Supporting Information, Figure 6). The similar applies to docking results as well (not shown). Thus, neither HB network nor SC contacts control the binding affinity of acridine derivatives to lysozyme.

*Role of van der Waals and Electrostatic Interactions.* To examine additional factors that could influence the binding, interaction energy between the ligand and the receptor was calculated using configurations obtained by the PM6-DH+ method. The computation was carried out for AMBER 99SB[30] force fields within Amber11 suit. Supporting Information, Figure S7, shows that van der Waals (vdW) interactions slightly dominate over electrostatic interactions for ligands I1, S2, and I2. On the other hand, the contribution of electrostatic energy strongly affects interaction of the ligands C1, T1OH, and C2OH with the receptor. For the remaining ligands, contributions of two interactions are comparable. Thus, the impact of vdW and Coulomb interactions on the binding affinity depends on the ligands.

The contributions of the core, linker, and side chains to the binding energy are shown in the Supporting Information, Figure S8. Interestingly, the electrostatic interactions between the core and receptor were always repulsive. This was also true for the side chains except T1OH and S2, where a very weak attraction was observed. The electrostatic interaction of the linker dominated for all ligands, while the vdW interactions with side chain dominated in most cases (Supporting Information, Figure S8). It should be noted that there was no correlation between vdW interactions of all three parts of the ligand and the IC$_{50}$ (Supporting Information, Figure S9). However, the electrostatic interactions of the core and linker highly correlated with the IC$_{50}$, while weaker correlation was seen for the side chains (Supporting Information, Figure S10). We conclude that the relative binding affinity of acridine derivatives seems to be mainly dependent on the electrostatic interaction.

*Binding Site is Positively Charged.* As shown in the Supporting Information, Figure S11, the core and the side chain of all ligands are positively charged, while the linker charge is

negative. Because the charge of the binding site is positive, the electrostatic interaction with the core is repulsive (Supporting Information, Figure S11) the charge of the binding site is positive. The positive charge of binding site can be seen also from contributions of the side chain and linkers.

*Detailed Explanation of Differences in Binding Affinity.* Our experiments and PM6-DH+ calculations suggest that ligands T1, T2, C1, and C2 are the best binders. High binding affinity of C1 and C2 can be explained by the presence of a rigid ring within the linker which reduces the entropy and leads to an increase of the binding free energy. The reason of higher binding affinity of T1 and T2, compared to S2, with a very weak binding, is undoubtedly associated with replacement of the thiocarbonyl group in the linker of T1 and T2 with the carbonyl group in semicarbazide S2. From the conventional point of view, the O atom is more electronegative than sulfur, and should increase the negative charge of the semicarbazide linker compared to thiosemicarbazide. Thus, the replacement of the C=S by C=O group should enhance the binding affinity to the positively charged lysozyme binding site. However, this is not the case. It is well-known, from NMR data and $pK_a$ values, that NH protons surrounding the C=X group (X = S or O) in thioureas are more acidic than in ureas because of specific sulfur properties. Thus, the C=S group in thiosemicarbazide is a stronger electron-withdrawing moiety than the carbonyl group in semicarbazide. This difference, apparently, does not influence the negative charge of the linker, as suggested by the data in the supplemental Table S1, where the charges on linkers in T1, T2, C1, and C2 are almost the same, about −0.66 e. The replacement of C=S by C=O has a greater effect on positive acridine charges which decrease by 0.020−0.046 e and sugar charges which increase by 0.030−0.035 e. Apparently, the observed biological activity cannot be explained simply by the charges of three constituting units of glyco-conjugates.

We next considered resonance effects in the valence bond theory.[61] T2 and S2 molecules are stabilized by the overlap of nonbonded p-orbital of N2 with π-orbital of C27=S and C27=O9, respectively (Supporting Information, Figure S12). A lone pair of electrons of N2 is partially transferred to the π-orbital, but the amount of transferred charge depends on the volume of overlap. Therefore, it depends on how much of the π-orbital is localized on C27. According to the Valence Bond theory, a π-bond of C is formed by overlapping 2p-orbital of C with 2p-orbital of O in C=O group and 3p-orbital of S in C=S group. Because the overlap of 2p-orbital with 2p-orbital is more efficient than with 3p-orbital, and the 2p-orbital of O has lower energy than 3p-orbital of S, the π-orbital is more localized on C in C=S than C in C=O. This means that the amount of N2 electron transferred to C27 in T2 is more than to C27 in S2. Therefore, N2 in T2 is more potent in withdrawing electron from N1 and the core part. This idea can be proven quantitatively by considering charge of the individual atoms in the linker group (Supporting Information, Table S2) as well as the geometry of N2 with its bonded atoms within T2 and S2 (Supporting Information, Figure S12). The geometry of N2 with its three bonded atoms should be more planar and the three angles should be closer to 120° (closer to sp$^2$ than sp$^3$ hybridization) if the overlap of nonbonded p-orbital of N2 with π-orbital is more effective.

Although T1OH and C2OH have the same linker as T1 and C2, their IC$_{50}$ values are considerably higher than those of T1 and C2 because their deacetylated saccharide unit has lower number of atoms reducing the van der Waals interaction.

Charges of the core group of isothiosemicarbazides I1 and I2 are smaller than those of T1 and T2 (Supporting Information, Table S1) and their linker is the most flexible. This explains why I1 and I2 have higher IC$_{50}$ values than T1 and T2. Thus, the IC$_{50}$ values increase with the decrease of the electrostatic interaction (or decrease of charge) of the core group (Supporting Information, Figure S10).

## 4. CONCLUSION

In the present study, we investigated the interference of glyco-acridines with the amyloid fibrillization of lysozyme in vitro. We have found that the ability to inhibit lysozyme fibrillization and depends on the structure of acridine derivatives.

Our data indicate that planarity of the acridine core ring is important but not the sole parameter affecting the inhibitory activity of the compounds. The linker and the saccharide type also affect the activity. Using the valence bond theory, one can explain differences in the effect of carbonyl versus thiocarbonyl moiety within the linker on the charge of the ligand. Contrary to the conventional point of view, thiocarbonyl reduces the charge to a greater extent than does the carbonyl group, which may be a reason for lower IC$_{50}$ value of T2 compared to S2. Comparison of binding energies obtained from docking with those obtained by PM6-DH+ method points to the importance of contribution of quantum effects to the binding affinity of glyco-acridines to lysozyme. Interestingly, we found that hydrogen bonding is not the key factor controlling the binding affinity and the extent of the role of van der Waals and electrostatic interactions depends on ligands.

For the most effective inhibitors, T1, T2, C1, and C2 the IC$_{50}$ values were at (sub)micromolar level. These features entitle glyco-acridine conjugates to be considered as potential therapeutic agents against diseases associated with the lysozyme amyloid aggregation and amyloid-related diseases in general.

## ■ ASSOCIATED CONTENT

**Ⓢ Supporting Information**

Additional figures and tables. This material is available free of charge via the Internet at http://pubs.acs.org.

## ■ AUTHOR INFORMATION

**Corresponding Author**

*E-mail: gazova@saske.sk.

**Notes**

The authors declare no competing financial interest.

## ■ ACKNOWLEDGMENTS

## ■ REFERENCES

(1) Aguzzi, A.; O'Connor, T. *Nat. Rev. Drug Discovery* **2010**, *9*, 237−248.

(2) Uversky, V. N.; Fink, A. L. *Biochim. Biophys. Acta* **2004**, *1698*, 131−153.

(3) Stefani, M. *Biochim. Biophys. Acta* **2004**, *1739*, 5−25.

(4) Dobson, C. M. *Semin. Cell Dev. Biol.* **2004**, *15*, 3−16.

(5) Winner, B.; Jappelli, R.; Maji, S. K.; Desplats, P. A.; Boyer, L.; Aigner, S.; et al. *Proc. Natl. Acad. Sci. U.S.A.* **2010**, *108*, 4194−4199.

(6) Baglioni, S.; Casamenti, F.; Bucciantini, M.; Luheshi, L. M.; Taddei, N.; Chiti, F.; Dobson, C. M.; Stefani, M. *J. Neurosci.* **2006**, *26*, 8160−8167.

(7) Cohen, F. E.; Kelly, J. W. *Nature* **2003**, *426*, 905−909.

(8) Hard, T.; Lendel, Ch. *J. Mol. Biol.* **2012**, *421*, 441−465.

(9) Estrada, L. D.; Soto, C. *Curr. Top. Med. Chem.* **2007**, *7*, 115−126.

(10) Porat, Y.; Abramowitz, A.; Gazit, E. *Chem. Biol. Drug Des.* **2006**, *67*, 27−37.

(11) Vieira, M. N.; Figueroa-Villar, J. D.; Meirelles, M. N.; Ferreira, S. T.; De Felice, F. G. *Cell Biochem. Biophys.* **2006**, *44*, 549−553.

(12) De Felice, F. G.; Houzel, J.; Garcia-Abreu, J.; Louzada, P. R.; Afonso, R. C.; Meirelles, M. L.; Lent, R.; Neto, V. M.; Ferreira, S. T. *FASEB J.* **2001**, *15*, 1297−1299.

(13) Latawiec, D.; Herrera, F.; Bek, A.; Losasso, V.; Candotti, M.; Benetti, F.; Carlino, E.; Kranjc, A.; Lazzarino, M.; Gustincich, S.; Carloni, P.; Legname, G. *PLoS One* **2010**, *5*, 9234.

(14) Gazit, E. *FASEB J.* **2002**, *16*, 77−83.

(15) Bemporad, F.; Taddei, N.; Stefani, M.; Chiti, F. *Protein Sci.* **2006**, *15*, 862−870.

(16) Tracz, S. M.; Abedini, A.; Driscoll, M.; Raleigh, D. P. *Biochemistry* **2004**, *43*, 15901−15908.

(17) Feng, B. Y.; Toyama, B. H.; Wille, H.; Colby, D. W.; Collins, S. R.; May, B. C. H.; Prusiner, S. B.; Weissman, J.; Shoichet, B. K. *Nat. Chem. Biol.* **2008**, *4*, 197−199.

(18) Sarkar, N.; Kumar, M.; Dubey, V. K.. *Biochim. Biophys. Acta* **2011**, *1810*, 809−814.

(19) De Felice, F. G.; Veira, M. N. N.; Nazareth, M.; Meirelles, L.; Morozova-Roche, L. A.; Dobson, C. M.; Ferreira, S. T. *FASEB J.* **2004**, DOI: 10.1096/fj.03-1072fje.

(20) Yang, F.; Lim, G. P.; Begum, A. N.; Ubeda, O. J.; Simmons, M. R.; Ambegaokar, S. S.; Chen, P. P.; Kayed, R.; Glabe, C. G.; Frautschy, S. A.; Cole, G. M. *J. Biol. Chem.* **2005**, *280*, 5892−5901.

(21) Ono, K.; Yamada, M. *J. Neurochem.* **2006**, *97*, 105−115.

(22) Wang, S. S. S.; Liu, K. N.; Lee, W. H. *Biophys. Chem.* **2009**, *144*, 78−87.

(23) Li, J.; Zhu, M.; Manning-Bog, A. B.; Di Monte, D. A.; Fink, A. L. *FASEB J.* **2004**, *18*, 962−962.

(24) Bahramikia, S.; Yazdanparast, R.; Gheysarzadeh, A. *Chem. Biol. Drug Des.* **2012**, 1−10.

(25) Cohen, T.; Frydman-Marom, A.; Rechter, M.; Gazit, E. *Biochemistry* **2006**, *45*, 4727−4735.

(26) Morshedi, D.; Ghaleh, N. R.; Habibi, A. E.; Ahmadian, S.; Gorgani, M. N. *FEBS J.* **2007**, *274*, 6415−6425.

(27) Gazova, Z.; Bellova, A.; Daxnerova, Z.; Imrich, J.; Kristian, P.; Tomascikova, J.; Bagelova, J.; Fedunova, D.; Antalik, M. *Eur. Biophys. J.* **2008**, *37*, 1261−1270.

(28) Antosova, A.; Chelli, B.; Bystrenova, E.; Siposova, K.; Valle, F.; Imrich, J.; Vilkova, M.; Kristian, P.; Biscarini, F.; Gazova, Z. *Biochim. Biophys. Acta* **2011**, 485−474.

(29) Bucciantini, M.; Giannoni, E.; Chiti, F.; Baroni, F.; Formigli, L.; Zurdo, J.; Taddei, N.; Ramponi, G.; Dobson, C. M.; Stefani, M. *Nature* **2002**, *416*, 507−511.

(30) Wang, W.; Nema, S.; Teagarden, D. *Int. J. Pharm.* **2010**, *390*, 89−99.

(31) Dobson, C. M. *Nature* **2003**, *426*, 884−890.

(32) Artymiuk, P. J.; Blake, C. C. *J. Mol. Biol.* **1981**, *152*, 737−762.

(33) Radford, S. E.; Dobson, C. M.; Evans, P. A. *Nature* **1992**, *358*, 302−307.

(34) Pepys, M. B.; Hawkins, P. N.; Booth, D. R.; Vigushin, D. M.; Tennent, G. A.; Soutar, A. K.; Totty, N.; Nguyen, O.; Blake, C. C. F.; Terry, C. J.; Feest, T. G.; Zalini, A. M.; Hsuan, J. J. *Nature* **1993**, *362*, 553−557.

(35) Dumoulin, M.; Kumita, J. R.; Dobson, C. M. *Acc. Chem. Res.* **2006**, *39*, 603−610.

(36) Frare, E.; de Laureto, P. P.; Zurdo, J.; Dobson, C. M.; Fontana, A. *J. Mol. Biol.* **2004**, *340*, 1153−1165.

(37) Kumar, S.; Ravi, V. K.; Swaminathan, R. *Proteins Proteomics* **2009**, *1794*, 913−920.

(38) Dolinsky, T. J.; Nielsen, J. E.; McCammon, J. A.; Baker, N. A. *Nucleic Acids Res.* **2004**, *32*, W665−W667.

(39) Sanner, M. F. *J. Mol. Graphics Mod.* **1999**, *17*, 57−61.

(40) Trott, O.; Olson, A. J. *J. Comput. Chem.* **2010**, *31*, 455−461.

(41) Morris, G. M.; Goodsell, D. S.; Huey, R.; Olson, A. J. *Mol. Des.* **1996**, *10*, 293−304.

(42) Morris, G. M.; Godsell, D. S.; Halliday, R. S.; Huey, R.; Hart, W. E.; Belew, R. K.; Ol- son, A. J. *J. Comput. Chem.* **1998**, *19*, 1639−1662.

(43) Shano, D. F. *Math. Comput.* **1970**, *24*, 647−656.

(44) Stewart, J. J. P. *J. Mol. Model.* **2009**, *73*, 765−805.

(45) Stewart, J. J. P. *Stewart Computational Chemistry*, 2011; http://openmopac.

(46) Korth, M. *J. Chem. Theory Comput.* **2010**, *6*, 3808−3816.

(47) Dobes, P.; Rezac, J.; Fanfrlik, J.; Otyepka, M.; Hobza, P. *J. Phys. Chem. B* **2011**, *115*, 8581−8589.

(48) Fanfrlik, J.; Bronowska, A. K.; Rezac, J.; Prenosil, O.; Konvalinka, J.; Hobza, P.. *J. Phys. Chem. B* **2011**, *114*, 1266−12678.

(49) Zhang W.; Hou T.; Schafmeister C.; Ross W. S. Case D. A. Leap and sleap. *AmberTools User's Manual*, 1st ed.; 2011.

(50) Klamt, A.; Schuurmann, G. *J. Chem. Soc., Perkin Trans.* **1993**, *2*, 799−805.

(51) Raghu, P.; Reddy, G. B.; Sivakumar, B. *Arch. Biochem. Biophys.* **2002**, *400*, 43−47.

(52) Porat, Y.; Abramowitz, A.; Gazit, E. *Chem. Biol. Drug Des.* **2006**, *67*, 27−37.

(53) Ghosh, S.; Pandey, N. K.; Dasgupta, S. *Int. J. Biol. Macromol.* **2013**, *54*, 90−98.

(54) Lemkul, J. A.; Bevan, D. R. *Biochemistry* **2010**, *49*, 3935−3946 (2010).

(55) Levy-Sakin, M.; Shreberk, M.; Daniel, Y.; Gazit, E. *Islet* **2009**, *1*, 210−215.

(56) Liu, K.-N.c; Lai, C.-M.; Lee, Y.-T.; Wang, S.-N.; Chen, R. P.-Y.; Jan, J.-S.; Liu, H.-S.; Wang, S. S.-S. *Biochim. Biophys. Acta* **2012**, *180* (11), 1774−1786.

(57) Sarkar, N.; Kumar, M.; Dubey, V. K. *Process Biochem. (Amsterdam, Neth.)* **2011**, *46*, 1179−1185.

(58) Scherzer-Attali, R.; Shaltiel-Karyo, R.; Adalist, Y.; Segal, D.; Gazit, E. *Proteins: Struct., Funct., Bioinf.* **2012**, *80*, 1962−1973.

(59) Rabiee, A.; Ebrahim-Habibi, A.; Navidpour, L.; Morshedi, D.; Ghasemi, A.; Sabbaghian, M.; Nemati-Lay, M.; Nemat-Gorgani, M. *Chem. Biol. Drug Des.* **2011**, *78*, 659−666.

(60) Gavrin, L. K.; Denny, R. A.; Saiah, E. *J. Med. Chem.* **2012**, *55*, 10823−10843.

(61) Cooper, D. L. *Valence Bond Theory*, 1st ed., Elsevier: Amsterdam, 2002.